www.amlett.com, www.vbripress.com/aml, DOI: 10.5185/amlett.2016.6103 Published online by the VBRI Press in 2016

Rapid synthesis and photoluminescent characterization of $MAl_2O_4:Eu^{2+}$, Dy^{3+} (M = Ca/Ca + Ba/Ca + Mg) blue nanophosphors for white lighting display applications

Devender Singh[1*,2], Vijeta Tanwar[1], Anura P. Simantilke[2], Bernabe Mari[3], Pratap S. Kadyan[1] and Ishwar Singh[1]

[1]*Department of Chemistry, Maharshi Dayanand University, Rohtak 124001, India*
[2]*Centro de Fisica, Universidade of Minho, Braga 4710057, Portugal*
[3]*Departament de Física Aplicada, Universitat Politècnica de València, València 46022, Spain*

[*]Corresponding author. Tel: (+91) 9896001262; E-mail: devjakhar@gmail.com

Received: 20 August 2015, Revised: 11 October 2015 and Accepted: 04 December 2015

ABSTRACT

The persistent $MAl_2O_4:Eu^{2+}$, Dy^{3+} (M may be Ca or Ca+Ba or Ca+Mg) blue light emitting nanophosphors were prepared by rapid facile gel combustion technique. For the syntheses of present series of phosphors, urea was used as an organic fuel and boric acid was used as a flux in presence of air. Photoluminescence properties were studied by excitation and emission spectra. The phosphors showed blue luminescence (λ_{max}= 454-458nm) under the excitation of UV source, attributed to $4f^6 5d^1 \rightarrow 4f^7$ transitions of the Eu(II) ion. The effect on photoluminescence intensity and decay time was also studied for varying metal ions in different ratio (Ca or Ca+Ba or Ca+Mg). The existence of divalent europium ions in the synthesized lattices was confirmed by the X-ray photoelectron spectroscopy. The crystal phase and size of the prepared materials were analyzed with X-ray diffraction patterns. The surface morphology of phosphors was studied with scanning electron microscopy and transmission electron microscopy techniques revealed the average size of the prepared materials between the 30-50 nm. The prepared nanophosphors had bright optoelectronic properties that could be efficiently applied in various solid state white light emitting display devices. Copyright © 2016 VBRI Press.

Keywords: Persistent phosphor; divalent europium; aluminate; photoluminescence property; combustion technique.

Introduction

Rare earth ions (RE) have received enormous attention due to unique electronic and optical characteristics developed from their 4f electrons. Rare earth ions doped host lattices capitulate efficient luminescent materials with high quantum yields, narrow bandwidth, host dependent luminescence sensitization and large strokes shift (useful in converting unusable ultraviolet light to useful visible light) [**1, 2**]. The interest for the lighting industry is evolving due to these aspects of rare earth activated light emitting materials. Particularly, rare earth activated light emitting phosphors find use in light emitting displays [**3**], bioimaging set-ups and solar cells [**4-6**]. Research on Eu^{2+} doped alkaline earth aluminate phosphors explains that these materials are having high quantum efficiency in the visible region [**7, 8**]. The long afterglow property shown by light emitting materials is generally considered as a destructive characteristic for conservative applications, e.g. in cathode ray tubes or in scintillators [**9**], luminous paint [**10**], luminous ceramics, textiles, the dial plate of watches and warning signs [**11, 12**].

Earlier used sulphide based (ZnS:Cu,Co) phosphor are sensitive towards the moisture, thus are chemically unstable. Presently aluminates phosphors are the best materials that have substituted the old sulfur containing commercial afterglow phosphors [**13, 14**]. $MAl_2O_4:Eu^{2+}$ materials are promising phosphors because they have good thermal and chemical stability as compared to sulfur based phosphors [**15, 16**]. Development in synthesis and characterization of alkaline earth aluminates especially $MAl_2O_4:Eu^{2+}$ and $MAl_{12}O_{19}:Eu^{2+}$ phosphors have resulted in significant interest in this class of materials [**17, 18**]. It is evident that the persistent luminescence of $MAl_2O_4:Eu^{2+}$ is improved to a great extent by codoping of some trivalent rare earth ions, e.g., Dy^{3+} and Nd^{3+} [**11**]. The Eu^{2+} ion acts as a luminescent center giving luminescence in the blue (λ_{max} = 440 nm) and green (λ_{max} = 520 nm) region for $CaAl_2O_4:Eu^{2+}$ and $SrAl_2O_4:Eu^{2+}$, respectively. The RE^{3+} (Nd and Dy) ions act as trap centre which enhanced the afterglow properties of phosphors.

The qualities of luminescent materials are mainly influenced by their synthetic technique. Since the long time,

aluminate luminescent materials were generally prepared by high temperature solid state reaction [**19-21**] and sol-gel process [**22, 23**]. But these methods are time consuming and need high temperature for processing of chemical reaction. Recently the combustion technique has shown characteristic advantages over other synthetic techniques i.e. low temperature required for their preparation, lesser reaction time, nano-sized particles formation of persistent phosphors [**11**, **24**].

Here in present work the luminescence and afterglow properties of $CaAl_2O_4:Eu^{2+}$, Dy^{3+}, $CaMgAl_2O_4:Eu^{2+}$,Dy^{3+} and $CaBaAl_2O_4:Eu^{2+}$, Dy^{3+} nanophosphors, prepared with the rapid gel combustion method, are investigated. The nanophosphors are synthesized to tune the color in europium doped materials with varying the ratios of alkaline earth metals. The effect of metal variation on photoluminescence intensity and decay time are also studied.

Experimental

Synthesis of nanophosphors

The powder samples with general formula $Ca_{(0.97)}Al_2O_4:Eu^{2+}$, Dy^{3+}, $Ca_{(0.47)}Mg_{(0.50)}Al_2O_4:Eu^{2+}$, Dy^{3+} and $Ca_{(0.47)}Ba_{(0.50)}Al_2O_4:Eu^{2+}$, Dy^{3+} (where Eu^{2+} =2 mole% and Dy^{3+} =1 mole%) were prepared by urea-nitrate rapid gel combustion method. Extra pure; $Ca(NO_3)_2.4H_2O$, $Ba(NO_3)_2$, $Mg(NO_3)_2.4H_2O$, $Al(NO_3)_3.9H_2O$, $Eu(NO_3)_3.6H_2O$, $Dy(NO_3)_3.6H_2O$, H_3BO_3 and $CO(NH_2)_2$ were weighed according to the stoichiometric proportion of above materials. Calculated amount of urea was used as a fuel [**25**] and boric acid was used as a flux as well as reducer. These starting raw materials were mixed with minimum amount of de-ionized water. Then the flux H_3BO_3 was added into the solution by varying 6 to 15 mole % of its molecular weight for each mole addition of europium. However the 10 mole % (of its molecular weight for each mole addition of europium) was found best in all prepared samples.

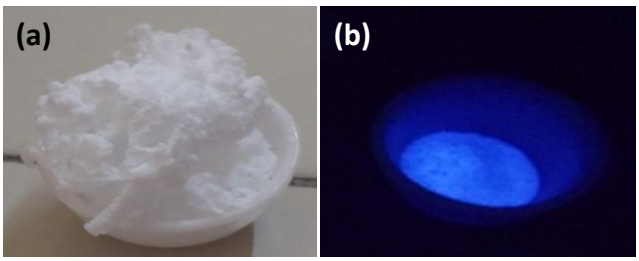

Fig. 1. Nanophosphor materials (a) as prepared without UV excitation, (b) with UV excitation (365nm).

Aqueous solution containing stoichiometric amounts of metal nitrates and urea was mixed by heating at 70 ^oC with constant stirring for making gel. Then mixture was introduced into a muffle furnace preset at 500 ^oC temperature. Within 5 minutes, the mixture formed froths and swelled forming foam, which caught fire. After the completion of process, crucible was removed out from the furnace. Upon cooling, fluffy material was obtained which showed blue luminescence under UV lamp as shown in **Fig. 1.** The concentration of the dopant (Eu^{2+}) was also varied from 0.5 to 6 mole %. However for the efficient photoluminescence properties the 2 mole % of dopant concentration was selected for further analysis. To see the effect of different alkaline earth metals on europium doped aluminate materials their different proportion was also tried. The synthesis of these materials is represented in chemical equation as follows:

$$[(1\text{-}x\text{-}z)M(NO_3)_2] + 2[Al(NO_3)_3.9H_2O] + [Eu(NO_3)_3.6H_2O] + z\,[Dy(NO_3)_2.6H_2O] + N_2H_4CO \longrightarrow M_{(1-x-z)}Al_2O_4:Eu_xDy_z + \text{Gaseous products } [N_2 + CO_2 + H_2O] \quad (1)$$

Characterization techniques

The phase purity was checked by using X-ray diffractometer (Rigaku Ultima IV X-ray diffractometer, using Ni-filtered Cu Kα1 radiation). The structural study was done by FTIR spectra of samples using a Nicolet 5700 infrared spectrometer. Phosphors were characterized for confirmation of oxidation state of europium with X-ray photoelectron spectroscope (Model/Supplier: PHI 5000 Versa Prob II). Optical characterization of the synthesized materials was carried out using Fluorimeter SPEX Fluorolog 1680 (USA) equipped with the SPEX 1934 D phosphorimeter having Xenon lamp as excitation source. The photoluminescence decay measurement was carried out by a photomultiplier tube (Hamamatsu R928). All the measurements were done at room temperature. The morphology of as prepared phosphors was inspected using a JEOL JSM-6360LV scanning electron microscope (SEM) and Hitachi F-7500 transmission electron microscope (TEM).

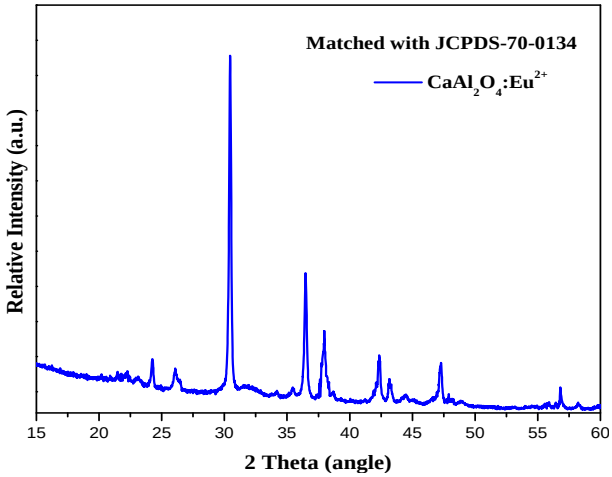

Fig. 2. X-ray diffraction patterns of the $CaAl_2O_4:Eu^{2+}$ nanophosphors.

Results and discussion

X-ray diffraction analysis

XRD patterns of the prepared materials were collected in 2θ range of 15-70^o for diagnosing the crystal phase. **Fig. 2-4** represents the XRD patterns of the products obtained using present fast gel combustion method. XRD pattern for Eu^{2+} doped $CaAl_2O_4$ (**Fig. 2**) is found crystalline and shows well resolved peaks corresponding to all the planes of standard monoclinic phase corresponding to JCPDS 70-0134.

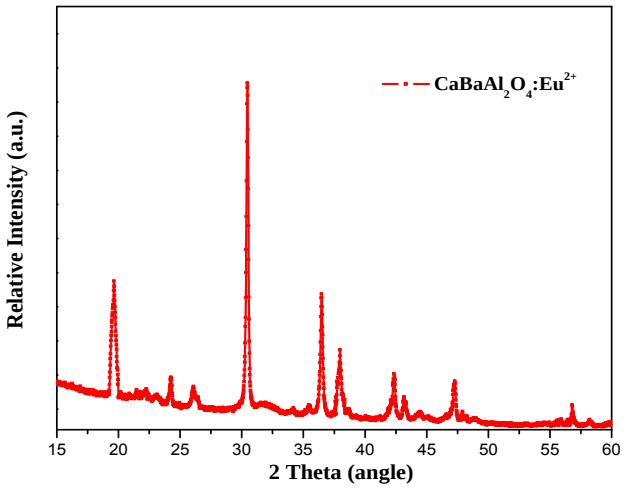

Fig. 3. X-ray diffraction patterns of the $CaBaAl_2O_4:Eu^{2+}$ nanophosphors.

Fig. 3 and **4** represent the X-ray diffraction patterns of divalent europium doped $CaBaAl_2O_4$ and $CaMgAl_2O_4$ phosphors respectively. The peaks of XRD pattern of $CaBaAl_2O_4$ are matching with $CaAl_2O_4$ (JCPDS. 70-0134) and $BaAl_2O_4$ (JCPDS 82-2001) lattices. While the peak position of XRD pattern of $CaMgAl_2O_4$ is matching with $CaAl_2O_4$ (JCPDS 70-0134) and $MgAl_2O_4$ (JCPDS 75-0905) lattices.

Here no phase transformations are observed after the addition of boric acid in sample as no extra peak appeared in their XRD patterns due to boric acid. However, when the H_3BO_3 content became higher than 15 % of the total lattice, in addition of major phase, one another phase was also obtained as a minor phase due to boric acid [**26**]. But here we have used boric acid is just 10 % (of its molecular weight for each mole addition of europium) so no additional phase is found.

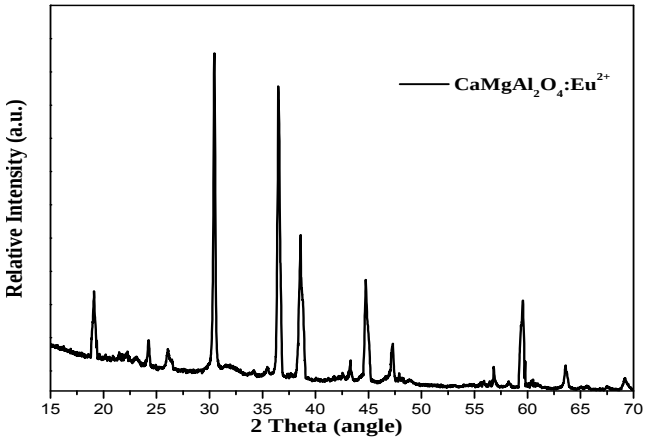

Fig. 4. X-ray diffraction patterns of the $CaMgAl_2O_4:Eu^{2+}$ nanophosphors.

A few XRD lines are present in doublet, which demonstrate that the lattice having two dissimilar lattice parameters, thus this suggest that the phase is changing from hexagonal phase to monoclinic phase. The doping of small amount of rare earth ions almost has no effect on lattice structure. The average crystallite size (D) of $CaAl_2O_4$ were estimated from the full width half maximum (FWHM) of the (220) diffraction peak of the powder by the use of Scherer's equation.

$$D = K\lambda/\beta\cos\theta \quad (2)$$

where, 'λ' is the X-ray wavelength (1.541 Ao), 'θ' is the Bragg's angle, 'k' is the constant depending on the particle's shape.

The calculated average sizes of particles of the synthesized phosphors are obtained in the range of 30-45 nm. The value of 2θ, full width half maxima and calculated average sizes for all the prepared phosphor particles are shown in **Table 1**.

Table 1. Represents the emission peaks and color coordinates of synthesized phosphors.

S. No.	Lattices	Emission peaks	Color co-ordinates
a	$CaAl_2O_4$:Eu,Dy	454.30	x-0.2023, y-0.0675
b	$CaBaAl_2O_4$:Eu,Dy	457.51	x-0.1568, y-0.0984
c	$CaMgAl_2O_4$:Eu,Dy	458.01	x-0.1894, y-0.1024

FTIR studies

The FTIR spectra of the series of phosphors were taken in the 4000–400 cm^{-1} region and are illustrated in **Fig. 5**. Antisymmetric stretching and antisymmetric bending appeared at 822 and 500 cm^{-1} respectively. Bands ranging from 400 to 600 cm^{-1} originated due to metal to oxygen (M-O) groups. The bands at 665, 457 and 420 cm^{-1} accredited to the stretching vibration of the Ca-O bond. Absence of O-H peaks indicated the good crystallinity of the prepared materials.

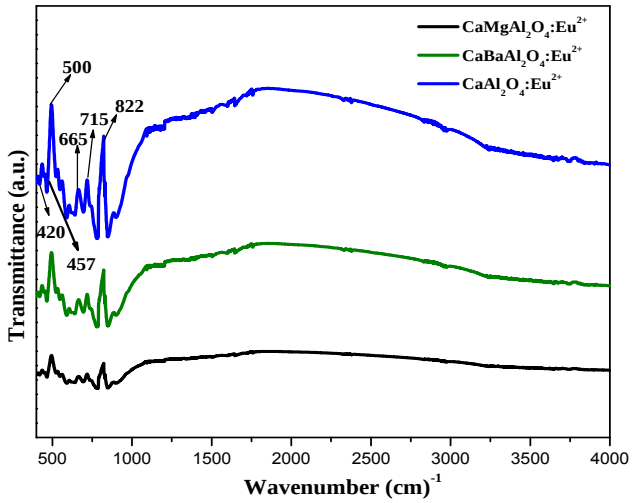

Fig. 5. FT-IR study of prepared phosphors.

X-ray photoelectron analysis

The elemental composition of the Eu^{2+} doped aluminate series of phosphors was analyzed by X-ray photoelectron spectroscopy as shown in **Fig. 6**. Phosphors were characterized here by the XPS for the confirmation of oxidation states of existing europium ions. Peaks of the all the constituents of synthesized phosphors were reliable with standard corresponding values of intensity of peaks. The peaks consequent to Eu (3d), Ca(2p), Ba (3d), Mg (2p), O (1s) and Al (2p) core levels were recognized in XPS spectra. The two peaks obtained at 51.2 eV and 531.8 eV indicate the Mg (2p) and O (1s), correspondingly [**27**]. The

Al (2s), Al (2p), Ca(2p3/2) and Ba $3d_{5/2}$ were situated nearly at 133 eV, 89.1 eV, 349.2 eV and 783.6 eV respectively. The peak at 1126.4 eV was due to the Eu^{2+} ($3d_{5/2}$) and the peak at 1153.4 eV originated from Eu^{2+} ions was ascribed to the Eu^{2+} ($3d_{3/2}$), if europium would be present in trivalent state then $3d_{5/2}$ and $3d_{3/2}$ peaks were found nearly at 1134 and 1165 eV respectively [**28**-**30**] but these peaks were absent in spectra, so this confirms the existence of divalent oxidation state of europium ions in these prepared lattices.

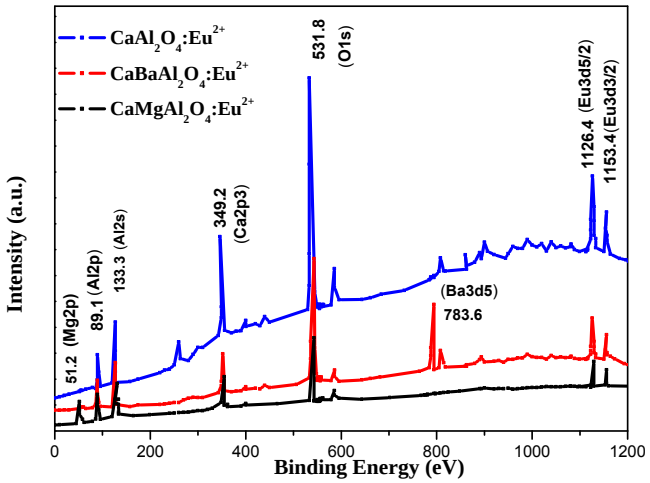

Fig. 6. XPS analysis of the prepared phosphors.

Optical properties

The photoluminescence emission spectra of phosphors along with excitation spectrum (inset) are shown in **Fig. 7**. Excitation peak was obtained at λex = 336 nm having a broad band from 280-400 nm. As shown in **Fig. 7** the emission spectra (λ_{em} = 454-458 nm) show a broad band emission attributed to $4f^65d^1 \rightarrow 4f^7$ transition of the Eu^{2+} showing blue luminescence which is found reliable to the literature [**31**]. The feature of a typical broad band emission in the visible light range indicates that the used activator (Eu) exist in divalent (Eu^{2+}, $4f^65d^1 \rightarrow 4f^7$ blue emission) rather than trivalent (Eu^{3+}, 4f→4f red, emission) which is based on the interaction of the matrix and the activator ion. It is considered that the major luminescent spectrum of 5d-4f transition in the Eu^{2+} ion is rarely influenced by introduction of the Dy^{3+} activator ion into the matrix. The lattices form three dimensional compact structures of tetrahedral in monoclinic aluminate structures. The Fuel and flux both act as reducing agent and the compact tetrahedral aluminate lattices protect itself from the attack of oxygen on Eu^{2+} ions in non-reducing atmospheric conditions. The reduction of $Eu^{3+} \rightarrow Eu^{2+}$ also could occur in non-reducing atmosphere due to the presence of borate tetrahedral anion group [**32, 33**], on addition of boric acid. The borate tetrahedral anion groups possibly transfer an electron for the reduction process of $Eu^{3+} \rightarrow Eu^{2+}$. As [$BO_4$] is having small size than [AlO_4] so electron density exist more on borate ions and because of the unstability due to more electron density and small size, it is possible to transfer electrons from borate ions to trivalent europium ions.

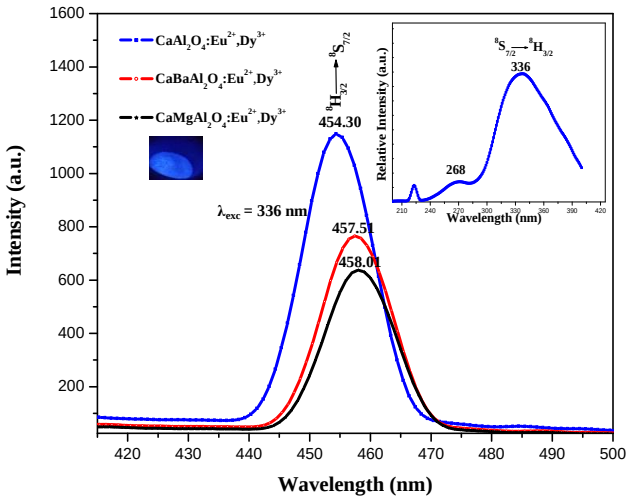

Fig. 7. PL emission spectrum and excitation spectrum (inset) of prepared phosphors.

In prepared phosphors lattices Mg^{2+}, Ca^{2+} and Ba^{2+} ions are having radii 0.072, 0.114 and 0.147 nm respectively. As Ca^{2+} ion is having slightly smaller size than Eu^{2+}, thus Ca^{2+} ions can be suitably substituted by Eu^{2+} ions but lattice will be slightly distorted. The radius of Ba^{2+} is larger than that of Eu^{2+} (0.125 nm), on replacing Eu^{2+} in the Ba^{2+} site, consequently the crystal field is distorted. As Mg^{2+} (0.072 nm) is having large ionic difference due to having enough small size in comparison to Eu^{2+}, so there is less possibility of substitution of Mg^{2+} by Eu^{2+}. So there is more substitution of Ca^{2+} and Ba^{2+} sites by Eu^{2+} ions in $CaAl_2O_4:Eu^{2+},Dy^{3+}$ and $CaBaAl_2O_4:Eu^{2+},Dy^{3+}$ phosphors in comparison to $CaMgAl_2O_4:Eu^{2+},Dy^{3+}$. However, the photoluminescence intensity of $CaAl_2O_4:Eu^{2+},Dy^{3+}$ phosphor is found highest in comparison to rest of other prepared phosphors because of formation of only single monoclinic phase as shown by XRD patterns. As monoclinic phase have perfect tetrahedral compact AlO_4 structures so there can occur efficient reduction of Eu^{3+} to Eu^{2+} resulting high photoluminescence intensity. Thus the highest photoluminescence intensity is obtained in $CaAl_2O_4:Eu^{2+}$, Dy^{3+} phosphor. $CaBaAl_2O_4:Eu^{2+}$, Dy^{3+}, $CaMgAl_2O_4:Eu^{2+}$, Dy^{3+} phosphors showed lower intensity due to non-formation of perfectly tetrahedral structures because of availability of two different metal aluminate lattices.

Table 2. All the decay parameters for the phosphors prepared with the present technique.

Phosphor compounds	A_1	τ_1 (min)	A_2	τ_2 (min)	τ_{avg} (min)
$CaAl_2O_4:Eu^{2+},Dy^{3+}$	1.81E+06	30.02374	4.53E+04	68.58428	32.6
$CaBaAl_2O_4:Eu^{2+},Dy^{3+}$	1.43E+09	27.77167	2.02E+06	50.66576	27.8
$CaMgAl_2O_4:Eu^{2+},Dy^{3+}$	1.25E+09	24.34167	1.92E+06	48.66376	24.4

Colorimetric parameters such as color coordinates and color ratios are constructive in signifying the emission color. This in turn is useful in determining the applicability of the phosphors in light emitting applications. **Table 2** provides a summary of the CIE coordinates of nanophosphors synthesized by rapid facile gel combustion method. The color coordinates are determined by using

emission spectra measured with excitation of 336 nm (**Fig. 8**). The most important result here is that the purity of blue emission seems to improve with increase of Ca ratio in $CaAl_2O_4:Eu^{2+}$, Dy^{3+}. Hence by increasing proportion of calcium, we tune the color from impure blue to pure blue.

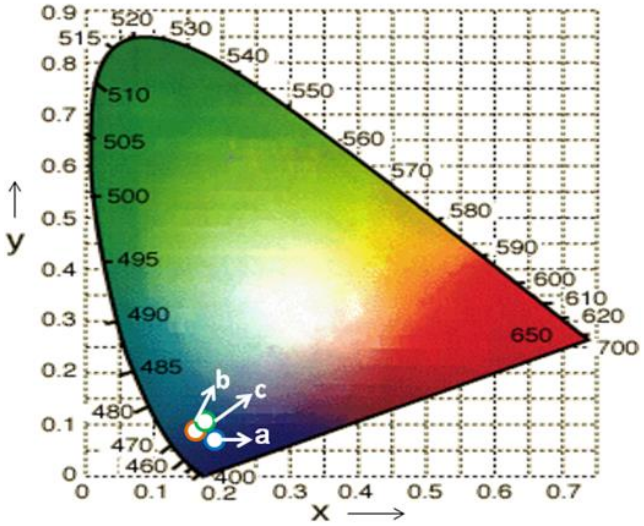

Fig. 8. Chromaticity diagram showing color coordinates of phosphors (a) $CaAl_2O_4$:Eu, Dy (b) $CaBaAl_2O_4$:Eu,Dy (c) $CaMgAl_2O_4$:Eu, Dy.

Decay analysis

The graph showing decay curves is presented in **Fig. 9**. It is taken after removing of the excitation source subsequent to 10 minutes irradiation continuously. The curves are showing long phosphorescence. The decay of the prepared phosphor materials were analyzed by the following second order decay equation [**34**]:

$$I = I_0 + A_1 \exp(-\tau/\tau_1) + A_2 \exp(-\tau/\tau_2) \quad (3)$$

where, I is the phosphorescence intensity at any time t after switching off the UV lamp, I_0, A_1, A_2 are the constant and τ_1, τ_2 are decay times for the exponential components of the study of the material.

The fitting results of all the parameters are listed in **Table 3.** The observed trend showed that the decay time of the phosphors decrease with the decrease of Ca metal ions proportion in prepared $MAl_2O_4:Eu^{2+}Dy^{3+}$ lattice. Diverse decay components are dependent on the charge carriers i.e., electrons and/or holes, produced on excitation, trapped at different trapping level, as the trap depth influenced the recombination of the excited electron and trapped hole to a great extent. After removing UV excitation source, the trapped holes probably liberated thermally to the valence band and migrated to recombine with excess electrons in metastable state sites leading to the long afterglow of the luminescence of these materials. Trapped holes shows longer lifetime when required thermal energy for detrapping is very high. Thus, longer decay times can be due to the higher density of deeper trap levels.

The average decay lifetime was calculated from the following equation [**35**]:

$$\tau_{avg} = (A_1 \tau_{12} + A_2 \tau_{22}) / (A_1 \tau_1 + A_2 \tau_2) \quad (4)$$

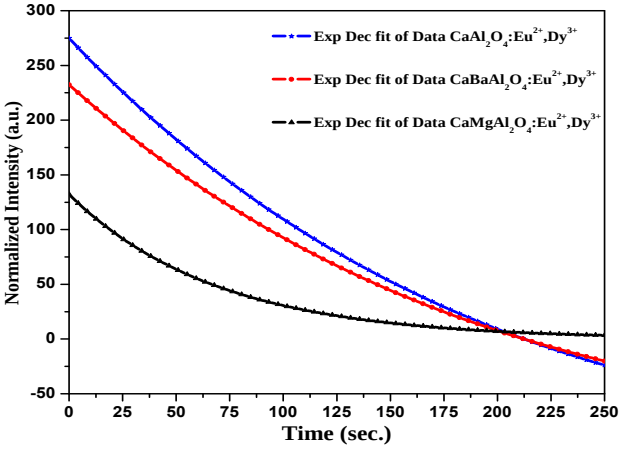

Fig. 9. Decay graph showing decay rate of different phosphors.

All the decay parameters of the phosphors prepared with present method are presented in **Table 3.**

Table 3. Crystallite sizes of prepared nanophosphors.

Phosphor materials	2 θ value (°)	FWHM (radian)	Particle size (nm)
$CaMgAl_2O_4:Eu^{2+}$	30.461	0.003822	42.0944
$CaAl_2O_4:Eu^{2+}$	30.461	0.005128	31.1182
$CaBaAl_2O_4:Eu^{2+}$	30.461	0.005313	30.3420

Morphology of phosphors

The surface of combustion foam were having many cracks, voids and pores due to the gasses released during the combustion reaction as shown in SEM images (**Fig. 10**). The combusted particles showed a very thin flake shape. These samples were having disconnected structures and foamy particles with different porosity. The observed morphology is reliable with other reports available on combustion consequent products [**36**]. In general, highly porous structures with large voids were observed for fuel rich samples. These pores and voids were expected because the large number of moles of gaseous products liberated through the network of lattice.

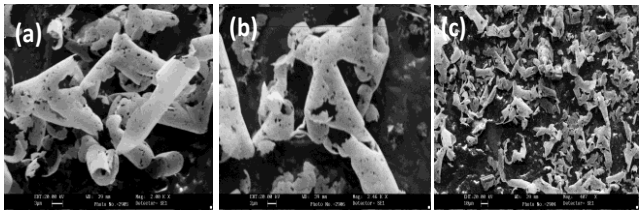

Fig. 10. SEM images of synthesized powders (a) $CaAl_2O_4$:Eu,Dy (b) $CaBaAl_2O_4$:Eu,Dy (c) $CaMgAl_2O_4$:Eu,Dy.

Transmission electron micrographs of the synthesized powders showed exceedingly agglomerated crystalline particles of nano size. TEM images of all the prepared samples were taken which are presented in **Fig. 11**. The synthesized samples showed aggregates of particles of spherical shape having sizes in the range of 30-50 nm. The particle size assessment from TEM studies were found in good concurrence with the calculated size from the XRD patterns of the prepared sample using Scherrer's equation.

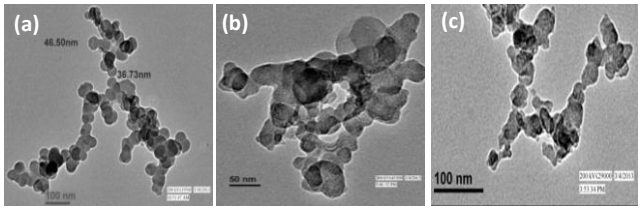

Fig. 11. TEM images of prepared powders (a) $CaAl_2O_4$:Eu,Dy (b) $CaBaAl_2O_4$:Eu,Dy (c) $CaMgAl_2O_4$:Eu,Dy.

Conclusion

The series of $MAl_2O_4:Eu^{2+}$, Dy^{3+} (M = Ca/Ca+Ba/Ca+Mg) phosphors were synthesized by rapid facile gel combustion technique. The photoluminescence emission spectra of synthesized phosphors showed a band at 454-458 nm with excitation of 336 nm radiations. Addition of Dy^{3+} helped in the improvement of the afterglow properties of prepared lattices. The effect on photoluminescence intensity and decay time was studied for varying metal proportion (Ca/Ca+Mg/Ca+Ba). It was observed that photoluminescence intensity was found highest in $CaAl_2O_4:Eu^{2+}Dy^{3+}$ phosphor material. The decay spectra showed the afterglow behavior of phosphors upto several minutes. CIE diagram illustrated the shifting of emissive color of phosphors towards the impure blue region with the replacement of half of calcium metal with magnesium or barium. XRD patterns showed that main diffraction peaks indexed well with monoclinic crystalline phase for $CaAl_2O_4:Eu^{2+}Dy^{3+}$. The particle size estimation from TEM studies was found in good agreement with the size estimated from XRD patterns using Scherrer's equation. The prepared nanophosphors had excellent optoelectronic properties that could be effectively used for various lightening optoelectronic devices.

Acknowledgements

The authors gratefully recognize the financial support from the University Grant Commission (UGC), New Delhi [MRP-40-73/2011(SR)] and the European Commission through Nano CIS project (FP7-PEOPLE-2010-IRSES ref. 269279).

Author contributions

Conceived the plan: DS, VT, IS; Performed the expeirments: DS, VT; Data analysis: DS, IS, APS, BM; Wrote the paper: VT,DS, IS, PSK. Authors have no competing financial interests.

Reference

1. Wong, H.T.; Tsang, M.K.; Chan, C.F.; Wong, K.L.; Fei, B.; Hao, J.; *Nanoscale*, **2013**, *5*, 3465. **DOI**: 10.1039/C3NR00081H
2. Kumar, N.; Kumar, V.; Swart, H.C.; Mishra, A.K.; Ngila, J.C.; Parashar, V.; *Mater. Lett.*, **2015**, *146*, 51. **DOI:** 10.1016/j.matlet.2015.01.150
3. Som, S.; Mitra, P.; Kumar, V.; Kumar, V.; Terblans, J. J.; Swart, H.C.; Sharma, S.K.; *Dalton Trans*., **2014**, *43*, 9860. **DOI:** 10.1039/c4dt00349g
4. Han, J.Y.; Im, W.B.; Kim, D.; Cheong, S.H.; Lee, G.Y.; Jeon, D.Y.; *J. Mater. Chem*., **2012**, *22(12)*, 5374. **DOI**: 10.1039/C2JM15501J
5. Krishna, R.H.; Nagabhushana, B.M.; Nagabhushana, H.; Murthy N.S.; Sharma S.C.; Shivakumara, C.; Chakradhar, R.P.S.; *J. Phys. Chem. C*, **2013**, *117*, 1915. **DOI**: 10.1021/jp309684b
6. Dorman, J.A.; Choi, J.H.; Kuzmanich, G.; Chang, J.P.; *J. Phys. Chem. C*, **2012**, *116*, 10333. **DOI**: 10.1021/jp300126r
7. Palilla, F.C.; Albere, A.K.; Tomkus, M.R.; *J. Electrochem. Soc. Solid State Scien.*, **1968**, *115*, 642. **DOI**: 10.1149/1.2411379
8. Som, S.; Kunti, A.K.; Kumar, V.; Kumar, V.; Dutta, S.; Chowdhury, M.; Sharma, S.K.; Terblans, J. J.; Swart, H.C.; *App. Phy*., **2014**, *115*, 193101. **DOI:** 10.1063/1.4876316
9. Blasse, G.; Grabmaier, B.C.; Luminescent Materials; Springer: Berlin, Germany, **1994**. **DOI**: 10.1007/978-3-642-79017-1
10. Murayama, Y.; Shionoya, S.; Yen, W.M.; In Phosphor Handbook; CRC Press: Boca Raton, FL, USA, **2007**, 651. **ISBN:** 13-978-0-8493-3564-8
11. Yamamoto, H.; Matsuzawa T.; *J. Lumin*., **1997**, *72-74*, 287. **DOI**:10.1016/S0022-2313(97)00012-4
12. Murayama, Y.; Takeuchi, N.; Aoki, Y.; Matsuzawa, T.; U.S. Patent 5424006, **1995**.
13. Sakai, R.; Katsumata, T.; Komuro, S.; Morikawa, T.; *J. Lumin.*, **1999**, *85*, 149. **DOI**:10.1016/S0022-2313(99)00061-7
14. Tsutai, I.; Kamimura, T.; Kato, K.; Kaneko, F.; Shinbo, K.; Ohta, M.; Kawakami, T.; *Electron. Eng. Jpn.*, **2000**, *132*, 7. **DOI**:10.1002/(SICI)1520-6416(20000715)132:13.0.CO;2-3
15. Cheng, B.; Zhang, Z.; Han, Z.; Xiao, Y.; Lei, S.; *Cryst. Eng. Commun*., **2011**, *13*, 3545. **DOI**:10.1039/C0CE00934B
16. Si, D.; Geng, B.; Wang, S.; *Cryst. Eng. Commun*., **2010**, *12*, 2722. **DOI**:10.1039/B921613H
17. Wiglusz, R.J.; Grzyb, T.; Lukowiak, A.; Bednarkiewicz, A.; Lis, S.; Strek, W.; *J. Lumin*., **2013**, *133*, 102. **DOI**:10.1016/j.jlumin.2011.12.039
18. Wiglusz, R.J.; Grzyb, T.; *Opt. Mater*., **2011**, *33*, 1506. **DOI**:10.1016/j.optmat.2011.04.020
19. Ju, S.H.; Kim, S.G.; Choi, J.C.; Park, H.L.; Mho, S.I.; Kim, T.W.; *Mater. Res. Bull.*, **1999**, *34*, 1905. **DOI**:10.1016/S0025-5408(99)00201-9
20. Lin, Y.; Zhang, Z.; Tang, Z.; Zhang, J.; Zheng, Z.; Lu, X.; *Mater. Chem. Phys*., **2001**, *70*, 156. **DOI**:10.1016/S0254-0584(00)00500-9
21. Nag, A.; Kutty, T.R.N.; *J. Alloys Compd.*, **2003**, *354*, 221. **DOI**:10.1016/S0925-8388(03)00009-4
22. Chen, I.C.; Chen, T.M.; *J. Mater. Res.*, **2001**, *16*, 644. **DOI**:10.1557/JMR.2001.0122
23. Peng, T.; Huajun, L.; Yang, H.; Yan, C.; *Mater. Chem. Phys.*, **2004**, *85*, 68. **DOI**:10.1016/j.matchemphys.2003.12.001
24. Peng, T.; Yang, H.; Pu, X.; Hu, B.; Jiang, Z.; Yan, C.; *Mater. Lett.*, **2004**, *58*, 352. **DOI**:10.1016/S0167-577X(03)00499-3
25. Ekambaram, S.; Patil, K.C.; Maaza, M.; *J. Alloys Comp.*, **2005**, *393*, 81. **DOI**:10.1016/j.jallcom.2004.10.015
26. Chen, J.; Gu, F.; Li, C.; *Cry. Growth & Design*, **2008**, *8*, 3175. **DOI**: 10.1021/cg700719h
27. Lee, S.M.; Ito, T.; Murakami, H.; in Proceedings of the Annual Autumn Conference on The Korea Institute of Electrical and Electronic Material Engineers, **2003,** 705.
28. Im, W.B.; Kang, J.H.; Lee, D.C.; Lee, S.; Jeon, D.Y.; Kang, Y.C.; Jung, K.Y.; *Solid State Commun*., **2005**, *133*, 197. **DOI**:10.1016/j.ssc.2004.10.016
29. Zhang, J.; Yang, M.; Jin, H.; Wang, X.; Zhao, X.; Liu, X.; Peng, L.; *Mater. Res. Bull.*, **2012**, *47*, 247. **DOI**:10.1016/j.materresbull.2011.11.015
30. Maślankiewicz, P.; Szade, J.; Winiarski, A.; Daniel, Ph.; *Cryst. Res. Technol.*, **2005**, *40*, 410. **DOI**: 10.1002/crat.200410359
31. Aitasalo, T.; Hölsä, J.; Jungner, H.; Lastusaari, M.; Niittykoski, J.; Parkkinen, M.; Valtonen, R.; *Opt. Mater.*, **2004**, *26*, 113. **DOI**:10.1016/j.optmat.2003.11.007
32. Pei, Z.; Su, Q.; Zhang, J.; *J. Alloys Compd*., **1993**, *198*, 51. **DOI**: 10.1016/0925-8388(93)90143-B
33. Zeng, Q., Pei, Z.; Su, Q.; *J. Alloys Compd.*, **1998**, *275*, 238. **DOI**:10.1016/S0925-8388(98)00311-9
34. Huang, C.H.; Chen, T.M.; *Opt. Express*, **2010**, *18*, 5089.

DOI: 10.1364/OE.18.005089.

35. Lee, G.; Im, W.B.; Kirakosyan, A.; Cheong, S.H.; Han, J.Y.; Jeon, D.Y.; Opt. Express, **2013**, *21*, 3287.
DOI: 10.1364/OE.21.003287
36. Patil, K.C.; Hegde, M.S.; Rattan, T.; Aruna, S.T.; Chemistry of Nanocrystalline Oxide Materials Combustion Synthesis Properties and Applications, World Scientific, **2008**.
DOI: 10.1142/6754

Supporting information

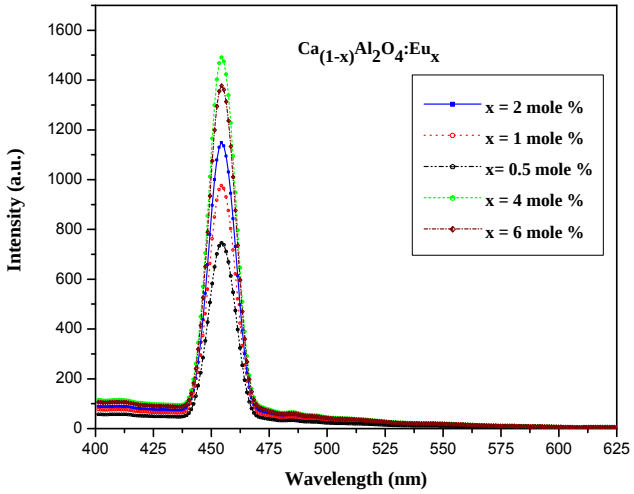

Fig. 1S: Photoluminescence spectra of the $CaAl_2O_4:Eu^{2+}$ nanophosphors.

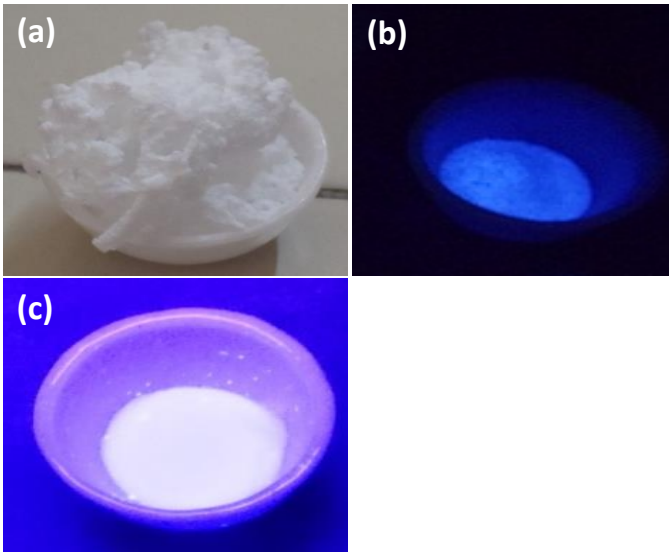

Fig. 2S: Nanophosphor materials (a) as prepared without UV excitation, (b) With UV excitation (365nm), (c) Crucible under UV light with white material.